Journal of Engineering and Applied Sciences 11 (12): 2769-2774, 2016
ISSN: 1816-949X
© Medwell Journals, 2016

Effect of Blade Tip Geometry on Centrifugal Compressor Performance and Stability

Ibrahim Shahin
Department of Mechanical Engineering, Shoubra Faculty of Engineering,
Benha University, Benha, Egypt

Abstract: The reliability operation for small fuel cells and hybrid fuel cell with gas turbine requires centrifugal compressor surge prevention. This study concerns a high speed centrifugal compressor stage with different blade tip geometries. The investigations were performed with unsteady three-dimensional, compressible flow simulations. A novel parameterization method has been developed to alter the tip geometry of an impeller blade. Different tip geometries are investigated includes flat tip blade, main blade winglet, main and splitter blade winglet and finally pressure side grooved tip. The performance and internal flow results are presented at surge, design and near choke points. The conclusion is that the tip geometry has a significant effect on the compressor performance and the operation stability at lower flow rates. The pressure ratio and surge margin for the blades with winglet have been improved and decreased for the grooved tip geometry. More uniform flow at impeller outlet with winglet blade. The use of winglet tip displaces the tip leakage vortex away from the blade and weakening the impingement effect. The winglet tip reduce the aerodynamic losses by unloading the tip section, reducing the leakage flow rate and turning the leakage flow in a more stream wise direction.

Key words: Blade tip, centrifugal compressor, performance and stability, surge, losses

INTRODUCTION

Centrifugal compressors are used in a wide variety of engineering applications for power generation and fuel cell is one of them. Fuel cell takes advantage of the electro-chemical reaction between oxygen and hydrogen to produce electricity. The compressor performance and stability has a big effect on the operation of the fuel cell. The Solid Oxide Fuel Cell (SOFC) integrated with a Gas Turbine (GT) has a potential for high efficiency electricity production with low environmental emissions. However, SOFC/GT hybrid systems face many challenges when it comes to load change and part-load operation. A gas turbine alone has good dynamic properties but part-load performance can be rather poor.

At any operation point, compressor surge must be prevented. Tip leakage flow is important for high speed transonic centrifugal compressor. The tip leakage flow has serious effect on the performance and stable operation. The effect is much more deleterious in centrifugal compressors than axial compressors because a centrifugal compressor has a long narrow flow passage so that the tip clearance occupies a large portion of the flow passage.

Tip leakage flow in centrifugal compressor has been studied by many researchers and its effect on the performance reduction is also investigated. The experimental and numerical studies of Lakshminarayana (1970), Moor *et al*. (1984), Farge *et al*. (1989), Hah (1986), Larosiliere and Skoch (1999) and Myong and Yang (2003) indicated that the leakage flow changes the behavior of secondary flow and the location of low momentum flow regions. The losses due to tip leakage flow reach 20-40% of the total losses. In fact, a review of the published work on tip leakage flow control reveals that centrifugal compressors and more generally radial machines have received much less attention than their axial counterparts in these areas, independently of the domain of application. The role played by tip leakage and blade tip geometry in axial turbomachines has received much attention, including axial compressors, turbines and fans. The experimental measurements by Inoue *et al*. (1986) show that the tip clearance has a big effect on the tip leakage flow characteristics. Furukawa *et al*. (1998) also studied the tip leakage vortex separation in axial flow compressor. The results indicated that a significant improve in the aerodynamic performance is resulted due to reducing the tip leakage mass flow rate.

Moore *et al*. (1984) investigated the effect of stationary casing treatment for axial compressors. The tip leakage flow is reduced with casing treatments. Pak performed detailed measurements on the complex flow field due to tip flow. Farge *et al*. (1989), Ishida *et al*. (1990) investigated the relative interaction between leakage flow, shock wave and boundary layer in a centrifugal compressor. The research performed by Barton *et al*. (2006), Ishida *et al*. (2005) and Dickmann *et al*. (2005) indicated that the casing treatment methods affect the performance of centrifugal compressor. The present study describes a study of the aerodynamic aspects of tip leakage flow in a centrifugal compressor with shroud less impeller. A numerical optimization process of different tip geometry is described. The way in which the geometry was parameterized and the way in which the optimization process was carried out was designed to reach several goals. The first goal was to gain more insight into the effect of the winglet on the flow physics and performance. The second was to investigate the trade-offs between the tip geometry effect on performance and its effect on the stable working rang of the centrifugal compressor. Tip leakage flow results in a considerable amount of aerodynamic loss in impeller flow field as discussed in the above section for the impeller with flat tip. One way of reducing tip losses is to use proper tip treatments. The specific tip treatments subject to investigation in this paper include special extensions of rotor tip winglet and tip grooves.

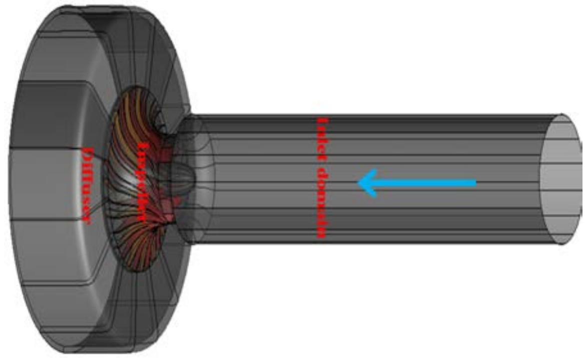

Fig. 1: Computational domain and flow path in the compressor stage

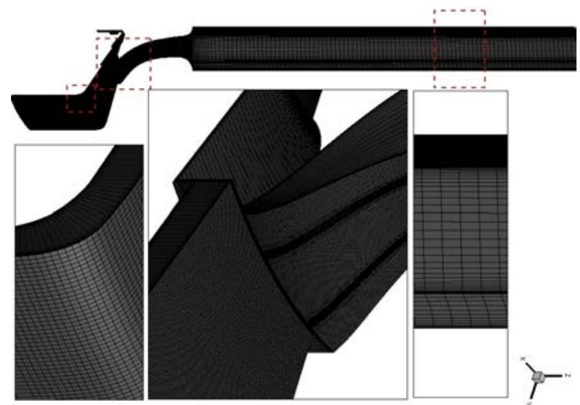

Fig. 2: Hexahedral meshes for the numerical domain

MATERIALS AND METHODS

Computational model: NASA CC3 vanless diffuser centrifugal compressor is studied by (McKain and Holbrook, 1997; Skoch *et al*., 1997). The numerical model divided into three parts; straight pipe inlet domain, semi open impeller and vaneless diffuser equipped with impeller hub side cavity region. The hub cavity flow is directed to labyrinth shaft seal. The inlet domain is extended for length equal to 5 times the compressor inlet diameter, to insure fully developed flow at inlet. The impeller out flow is moved to a vaneless diffuser with an annular radial-to-axial bend. The axial bend is extended more than the actual to minimize the effect of outlet boundary conditions on the flow inside the diffuser. The hub side cavity and shaft labyrinth seal are also modeled. Figure 1 shows the basic geometrical simulated domain for the moving and stationary parts.

Computational meshes: The structured hexahedral mesh is created using ICEM CFD 16 blocking tools the computational grid generated is shown in Fig. 2. In order to capture the boundary layer which is very important for compressor flows, the mesh is refined at the walls. The blade tip clearance is resolved with 10 cells in the radial direction. The grid is concentrated near the walls. The grid is enlarged by a ratio of 5% as moved far from the walls. Careful check for grid independence was also conducted; three numbers of computational nodes were checked and 3.23 million of nodes were used as no change in results with increasing the mesh nodes higher that number (Shahin *et al*., 2014). The numbers of nodes are changed by increasing the number of elements for the impeller and diffuser in meridional, radial and spanwise directions (Shahin *et al*., 2015).

Solver: Three-dimensional, Unsteady Reynolds-Averaged Navier-Stokes equations are solved for compressible flow. All of the numerical calculations were performed using FLUENT. A compressible, density based solver with SIMPLEC method for pressure-velocity coupling. The solved equations were discretized with second order of

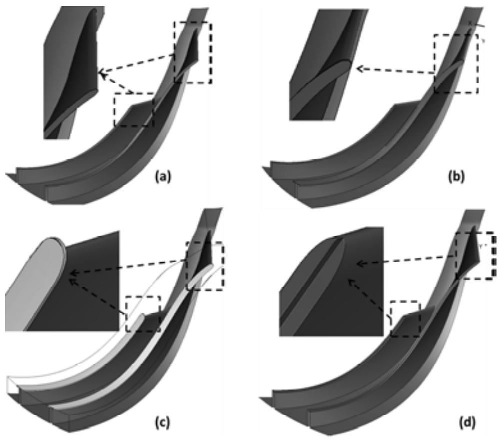

Fig. 3: Studied tip geometries: a) Flat blade tip; b) Winglet for main blades; c) Winglet for main and splitter blades; d) Blades with pressure side grooved tip

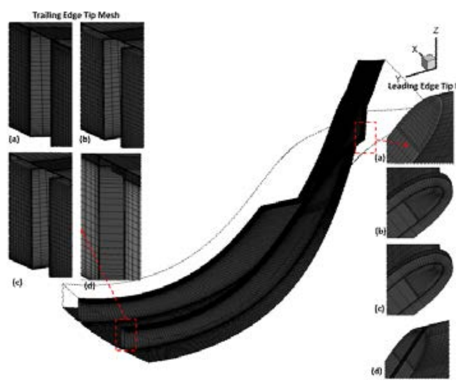

Fig. 4: Studied cases mesh: a) Flat blade tip; b) Winglet for main blades; c) Winglet for main and splitter blades; d) Blades with pressure side grooved tip

scheme. The sliding mesh is used for simulating the impeller rotation in which the multiple cell zones are connected to each other through interface boundary conditions. As the mesh motion is updated in time, the non-conformal interfaces are likewise updated to reflect the new positions of each zone. The interface between the moving and stationary parts is set to sliding Mesh in which the relative position is updated each time step. Although, the sliding mesh is computationally expensive while handling the rotation of the wheel but the wheel is actually rotating relative to the stationary compressor housing. Also, the blade passage effects are captured and the position of the rotating wheel relative to the diffuser is captured by which the relevant fluctuations are resolved. The turbulence is simulated by Renormalized Navier Stokes K-ε RNG turbulence model with non-equilibrium near wall treatments with 2% turbulence intensity at flow inlet. The discretization in space is of second order accuracy. The simulation was conducted on a server with 4 AMD Opteron processor, 48 cores and 128 GB of RAM. For the spatial discretization, a second order scheme was used. The second order implicit formulation was used for the temporal discretization. In order to resolve the relevant fluctuations, the grid resolution must be high with a small time step and the Courant number should be smaller than unity to be consistent with the flow properties which, for this case, gives a time step of 6.674e-6.

Boundary conditions: The mass flow inlet boundary condition is used at the inlet of the pipe, the inlet air was set at atmospheric pressure and 288 K, the interface boundary conditions are used at the interface between each rotating and stationary parts, the pressure outlet boundary conditions is used at the domain outlet. The computational domain is consist 24° sector to cover only one blade passage Fig. 2 and rotational periodic boundary condition was used to save the calculation time. The casing walls and blade surfaces were simulated with no slip wall boundary condition. The pressure outlet boundary condition is specified at the seal exit which equal to atmospheric pressure.

Tip treatment geometries: The investigated tip geometries included in this paper are flat blade tip, winglet for main blades, winglet for main and splitter blades and blades with pressure side grooved tip. The tip geometry and mesh are shown in Fig. 3 and 4, respectively.

RESULTS AND DISCUSSION

The pressure ratio variation with mass flow rate is shown in Fig. 5 for different tip blade geometries and compared with the base case with flat tip geometry. It can be seen that the pressure ratio for the cases with new tips has been increased except for the case with grooved blade tip. The surge inception mass flow rate is also decreased for the cases with using winglet but slightly increased for case with grooved tip. The surge margin for winglet tip cases has been improved due to the control of the tip vortex and higher stable mass flow due to the reduction of the tip mass flow rates. The choke flow limit is noticed to be decreased resulting from the area reduction due to the use of winglet. On the other hand, choke limit is slightly increased for grooved tip case

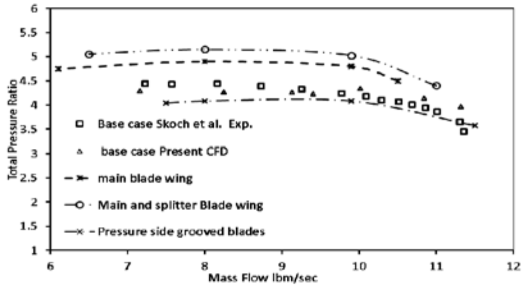

Fig. 5: Pressure ratio with mass flow rate for compressor with different tip geometries

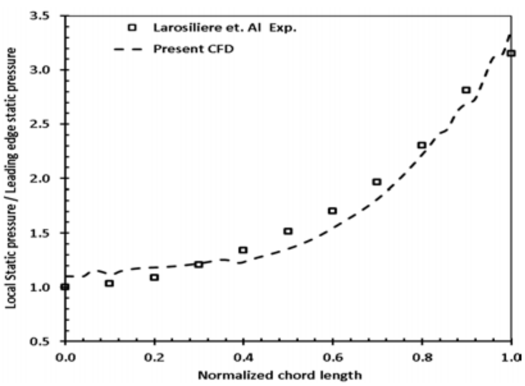

Fig. 6: Average static pressure distribution along the shroud for: a) Measured results of Larosiliere *et al.* (1997); b) Present CFD results

The pressure side grooved tip causes an increase for the flow area and also an increase for tip leakage flow.

In order to validate the pressure developed inside the impeller, the present CFD flow velocity is compared with Larosiliere *et al.* (1997). Figure 6 shows the static pressure rise along the shroud for the present CFD results and experimental results of Larosiliere *et al.* (1997) The area averaged static pressure from the present CFD agree well with the measurements till 30% of the chord length, after that the static pressure is slightly under estimated. This difference is due to the constant tip clearance used in Larosiliere *et al.* (1997).

In order to justify the improvement in the compressor pressure ratio, the developed pressure is averaged through the impeller and diffuser stream wise pass. Figure 7 shows the pressure along the compressor stage for different tip geometries, the horizontal axis represents the normalized length through the stream wise direction, point 0 represents the impeller inlet, point 1 represents the impeller outlet, point 1.4 represents the diffuser bend and diffuser outlet is represented by point The developed pressure through the impeller is enhanced when using winglet with higher enhancement for the case with winglet at the main blade. The use of winglet on main

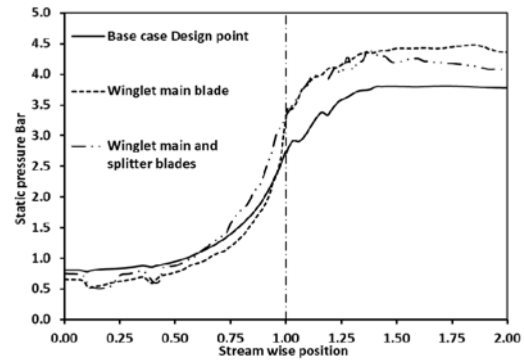

Fig. 7: Developed static pressure through the compressor stage for different tip geometries at design flow rate

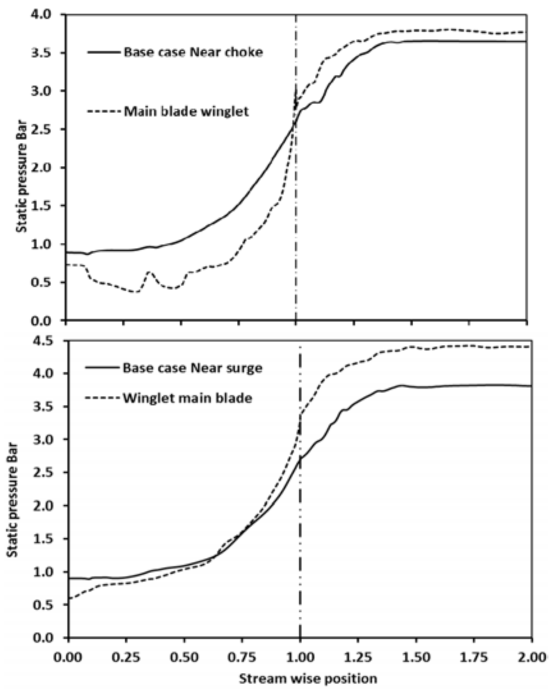

Fig. 8: Developed static pressure through the compressor stage at off design condition

and splitter blades also enhance the pressure ratio but an increase on the flow velocity results from the reduction in the flow area which will increase the friction losses through the impeller. case with main blade winglet at off design conditions. The pressure at the inducer area is decreased when compared with the case with flat tip, resulting from the increase of the velocity due to the reduction on the flow area. Contours of the radial normalized by the impeller tip speed are shown in Fig. 8 and 9 at the impeller exit plan for the base

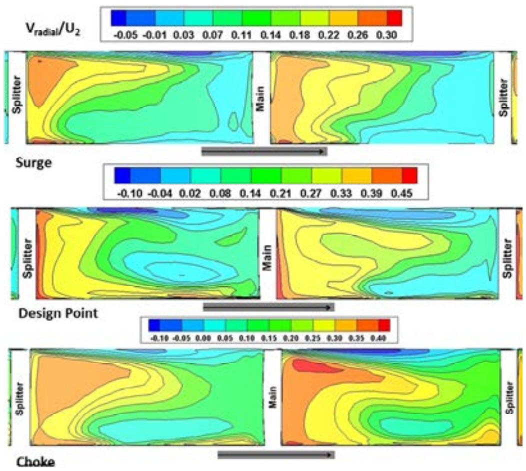

Fig. 9: Comparison of the radial velocity distributions normalized by the impeller tip speed at the impeller outlet

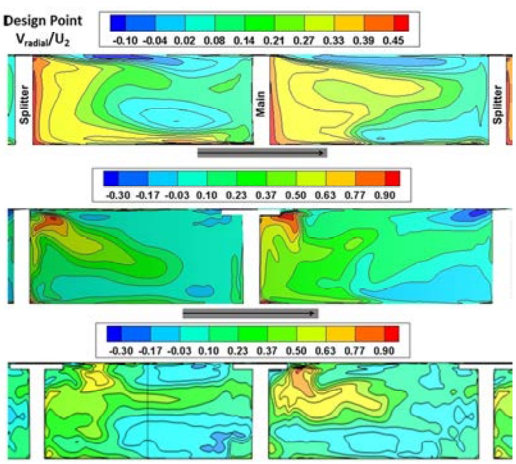

Fig. 10: Effect tip geometry on the radial velocity at impeller outlet for different tips

case at different operating point. Generally, near the suction side, low radial and high tangential velocities are found which agree with the classical jet-wake model. On the pressure side, the radial velocity is high while the tangential velocity is low. Close to the hub, the blade wake pattern can be identified as a region of lower radial velocity in the contour plot. The jet region is found close to the pressure side while the wake region has been established as a region of high absolute tangential velocity on the suction side. As the flow is reduced to near surge, high tangential velocities at mid-span and near the suction side of the blades. The jet appears as a region of low tangential velocities in the pressure side hub corner. As a result of flow through the tip clearance

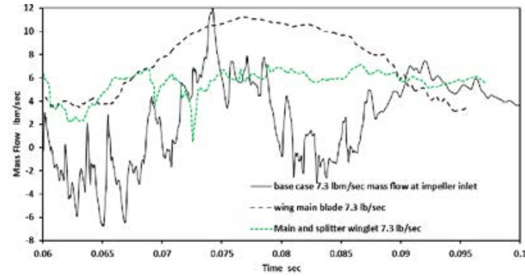

Fig. 11: Effect tip geometry on the impeller inlet mass flow stability at surge condition

low negative radial velocity region is detected near the shroud especially at low flow rate point, at which the blade wake and the jet interact strongly and interchange momentum. Near surge, stagnant or reversed flow is detected near the impeller shroud.

Figure 10 shows the radial velocity at impeller outlet for different tip geometries. Low momentum flow region caused by reversed secondary flow was observed at the blade suction side near the corner of impeller casing. When using winglet for the main or splitter blades, the velocity distribution at the impeller outlet is improved to be more uniform and the low momentum reverse flow region is disappeared and the effect of jet wake flow structure is decreased. The pressure ratio of both impellers with winglets higher than that of the impeller with flat tip, the reason for the pressure ratio improvement is that the reduction of the loss in the vanless diffuser parts due to a more uniform distribution of the velocity at the impeller outlet. The uniform velocity distribution near the corner of the impeller casing wall and the blade suction surface in the impeller with winglet tip is higher than that in the impeller with flat tip.

The mass flow at impeller inlet is shown in Fig. 11 with the flow time when working at surge flow rate. The base case with flat tip has the highest mass fluctuation with negative values which indicate the surge event existence. The stability is improved for cases with winglet tips and lowest fluctuations are detected for case with winglet tip for main and splitter blades.

CONCLUSION

The three dimensional URANS CFD simulation has been developed for high speed centrifugal compressor with a vanless diffuser. Different blade tips have been tested to improve the compressor performance and stability working range at lower flow rates. The flat blade tip, winglet main blade tip, winglet main and splitter tip and pressure side groove tips were studied numerically at different operating flow rates. The performance curves for the studied cases are presented and discussed. The average developed pressure through the impeller and diffuser were analyzed for all studied cases and different operating flow rates. Main results obtained and phenomena described in study indicates an improvement for the pressure ratio with winglet tip cases while a noticed decrease in developed pressure ratio with the use of grooved tip due to the increase of tip leakage flow. The base case with flat tip has the highest mass fluctuation with negative values which indicate the surge event existence. The stability at lower flow rates is improved for cases with winglet tips and lowest fluctuations detected case with winglet tip and splitter blades.

ACKNOWLEDGEMENTS

This publication was made possible by NPRP grant No. 4-651-2-242 from the Qatar National Research Fund (a member of Qatar Foundation). The statements made herein are solely the responsibility of the researchers.

REFERENCES

Barton, M.T., M.L. Mansour, J.S. Liu and D.L. Palmer, 2006. Numerical optimization of a vaned shroud design for increased operability margin in modern centrifugal compressors. J. Turbomach., 128: 627-631.

Dickmann, H.P., T.S. Wimmel, J. Szwedowicz, D. Filsinger and C.H. Roduner, 2005. Unsteady flow in a turbocharger centrifugal compressor: 3D-CFD-simulation and numerical and experimental analysis of impeller blade vibration. Proceeding of the ASME Turbo Expo 2005: Power for Land, Sea and Air, June 6-9, 2005, American Society of Mechanical Engineers, Reno, Nevada, ISBN:0-7918-4730-6, pp: 1309-1321.

Farge, T.Z., M.W. Johnson and T.M.A. Maksoud, 1989. Tip leakage in a centrifugal impeller. J. Turbomach., 111: 244-249.

Furukawa, M., M. Inoue, K. Saiki and K. Yamada, 1998. The role of tip leakage vortex breakdown in compressor rotor aerodynamics. Proceeding of the ASME 1998 International Gas Turbine and Aeroengine Congress and Exhibition, June 2-5, 1998, American Society of Mechanical Engineers, Stockholm, Sweden, ISBN:978-0-7918-7862-0, pp: 14-14.

Hah, C., 1986. A numerical modeling of endwall and tip-clearance flow of an isolated compressor rotor. J. Eng. Gas Turbines Power, 108: 15-21.

Inoue, M., M. Kuroumaru and M. Fukuhara, 1986. Behavior of tip leakage flow behind an axial compressor rotor. J. Eng. Gas Turbines Power, 108: 7-14.

Ishida, M., D. Sakaguchi and H. Ueki, 2005. Optimization of inlet ring groove arrangement for suppression of unstable flow in a centrifugal impeller. Proceeding of the ASME Turbo Expo 2005: Power for Land, Sea and Air, June 6-9, 2005, American Society of Mechanical Engineers, Reno, Nevada, ISBN:0-7918-4730-6, pp: 841-850.

Ishida, M., H. Ueki and Y. Senoo, 1990. Effect of blade tip configuration on tip clearance loss of a centrifugal impeller. J. Turbomach., 112: 14-18.

Lakshminarayana, B., 1970. Methods of predicting the tip clearance effects in axial flow turbomachinery. J. Basic Eng., 92: 467-480.

Larosiliere, L.M. and G.J. Skoch, 1999. Aerodynamic synthesis of a centrifugal impeller using computational fluid dynamics and measurements. J. Propul. Power, 15: 623-632.

Larosiliere, L.M., G.J. Skoch and P.S. Prahst, 1997. Aerodynamic Synthesis of a Centrifugal Impeller Using CFD and Measurements. National Aeronautics and Space Administration, Seattle, Washington, USA.,.

McKain, T.F. and G.J. Holbrook, 1997. Coordinates for a High Performance 4: 1 Pressure Ratio Centrifugal Compressor. NASA, Indianapolis, Indiana, Pages: 82.

Moore, J., J.G. Moore and P.H. Timmis, 1984. Performance evaluation of centrifugal compressor impellers using three-dimensional viscous flow calculations. J. Eng. Gas Turbines Power, 106: 475-481.

Myong, H.K. and S.Y. Yang, 2003. Numerical study on flow characteristics at blade passage and tip clearance in a linear cascade of high performance turbine blade. KSME Int. J., 17: 606-616.

Shahin, I., M. Gadala, M. Alqaradawi and O. Badr, 2014. Unsteady CFD simulation for high speed centrifugal compressor operating near surge. Proceeding of the ASME Turbo Expo 2014: Turbine Technical Conference on Exposition, June 16-20, 2014, American Society of Mechanical Engineers, Dusseldorf, Germany, ISBN:978-0-7918-4563-9, pp: 10-10.

Shahin, I., M. Gadala, M. Alqaradawi and O. Badr, 2015. Large eddy simulation for a deep surge cycle in a high-speed centrifugal compressor with vaned diffuser. J. Turbomach., Vol. 137, 10.1115/1.4030790

Skoch, G.J., PS. Prahst, M.P. Wernet, J.R. Wood and A.J. Strazisar, 1997. Laser anemometer measurements of the flow field in a 4: 1 pressure ratio centrifugal impeller. Proceeding of the ASME 1997 International Gas Turbine and Aeroengine Congress and Exhibition, June 2-5, 1997, American Society of Mechanical Engineers, Orlando, Florida, ISBN:978-0-7918-7868-2, Pages:13-13.